Spectroscopy of Hydrothermal Reactions 22. The Effects of Cations on the Decarboxylation Kinetics of Trifluoroacetate, Cyanoacetate, Propiolate, and Malonate Ions

Davide Miksa, Jun Li, and Thomas B. Brill*

Department of Chemistry and Biochemistry, University of Delaware, Newark, Delaware 19716

Received: April 10, 2002; In Final Form: September 17, 2002

The effect of Group 1 counterions on the decarboxylation rate of four carboxylate ions (trifluoroacetate, propiolate, cyanoacetate, and malonate) was determined in water at 140−280 °C and 275 bar. The decarboxylation kinetics were determined in real time by using IR spectroscopy and a titanium cell flow-reactor with sapphire windows. The complexity of the reaction of $CF_3CO_2^-$ necessitated additional postreaction studies by ^1H and ^{19}F NMR spectroscopy and F^- ion electrochemistry. Batch mode reactions in a titanium tube reactor were employed for the latter studies. The CF_3H product of $CF_3CO_2^-$ decomposed, liberating F^- ions. The cation effect for $CF_3CO_2^-$ is caused primarily by the reaction of F^- with the Group 1 cations in the order $Li^+ > Na^+ > K^+$..., which changed the ionic strength. The rate of decarboxylation of cyanoacetate was unaffected by the cation, whereas the Li^+ ion slowed the rate of decarboxylation of propiolate, perhaps because of complexation with propiolate. These results were compared with the previously investigated malonate system. Where a cation effect was observed, the effect could be attributed to some form of ion pairing, but in each case the details of the interaction differ slightly.

Introduction

One of the more important fundamental problems in hydrothermal chemistry is the effect of ionic substances on the reactions of other organic and inorganic compounds. Whether initially present or formed during a reaction, ionic substances are frequently major components of hydrothermal reactions in chemical processing and natural systems. Heavy emphasis has been placed on the thermodynamic properties of metal−organic systems,[1−3] with less emphasis on kinetics.[4,5] Thus, we have attempted to cast more light on the effect of cations and anions on the rates and pathways in selected hydrothermal reactions.

The intention was to determine the influence of the ionic potential (charge/size) of Group 1 cations ($M = Li^+$, Na^+, K^+, Rb^+, Cs^+) on the decarboxylation kinetics (reaction 1) of a series of carboxylate anions, $CF_3CO_2^-$, $NCCH_2COO^-$, $HCCCO_2^-$, and $HO_2CCH_2CO_2^-$. Real-time IR spectral measurements with a flow reactor were employed to compare the reaction rates.

$$M[RCO_2] + H_2O \rightarrow RH + CO_2 + M^+ + OH^- \qquad (1)$$

The $CF_3CO_2^-$ ion was perhaps the most unusual because the CF_3H product engaged in further hydrothermal reactions that produced F^- ions. The presence of M^+ and F^- ions in solution raised the ionic strength and caused an observable effect on the rate of reaction 1, except in the cases where ion pairing was the greatest.

The carboxylate ions containing the −CN and −CC− triple bonds in the backbone were investigated to explore the effect that the cation might have on possible resonance structures. The malonate ion has been discussed before,[6] and the effect of chelation of the cation on the decarboxylation rate of the anion was shown. In general, there appear to be many ways that the cations affect the decarboxylation rate, but all of the effects seem to fall under the umbrella of ion pairing.

Experimental Section

The trifluoroacetate salts, propiolic acid $HC{\equiv}CCO_2H$, cyanoacetic acid $N{\equiv}CCH_2CO_2H$, LiOH, NaOH, KOH, and 50% by wt aqueous RbOH and CsOH were obtained from Aldrich and used as received. The Milli-Q deionized water was sparged with compressed Ar to expel any gases before use. The aqueous propiolate and cyanoacetate solutions of Li^+, Na^+, K^+, Rb^+, and Cs^+ were prepared by titrating the acids with metal hydroxides in solution to the equivalence point. The $CF_3CO_2^-$ salts were studied at 0.25 *m* concentration, whereas the propiolate and cyanoacetate salts were studied at 0.5 *m* concentration.

The flow reactor and Ti cell (0.0819 cm^3) with sapphire windows used in the experiments have been described in detail elsewhere.[7,8] Several improvements[9,10] have automated the operation. This apparatus was used to study hydrothermal reactions in real time. The temperature range used was 140−280 ± 1 °C at a constant pressure of 275 ± 1 bar. The flow rates in the range of 0.10−1.00 ± 0.5% mL/min yielded residence times of 4.4−44.5 s.

A Nicolet 560 Magna FTIR spectrometer with an MCT-A detector was used for the transmission IR spectroscopy experiments involving the flow cell. For kinetics, the IR spectral measurements were recorded at 4 cm^{-1} resolution on 32 summed spectra. The total collection time for the summed spectra was approximately 10 s. All spectra were normalized with background spectra of pure water recorded at the same conditions. The asymmetric stretch of aqueous CO_2 at 2343 cm^{-1}, C≡C triple bond stretch at about 2090 cm^{-1}, and C≡N triple bond stretch in the region of 2254 cm^{-1} were all within the IR band-pass of sapphire and are useful for calculating the kinetics of decarboxylation based on the absorbance change.

* Corresponding author. E-mail: brill@udel.edu

10.1021/jp020941t CCC: $22.00
Published on Web 10/24/2002

The band areas of CO_2 were converted into concentrations by using the Beer−Lambert law with the previously determined molar absorptivity of aqueous CO_2.[11] During decarboxylation of the cyanoacetate ion, the C≡N stretch of the CH_3CN product of decomposition overlapped that of the reactant $NCCH_2CO_2^-$. The contribution of CH_3CN must, therefore, be subtracted from the band area of $NCCH_2CO_2^-$ when determining the concentration of the anion. This procedure is described in the following section. The weighted least-squares regression[12] was performed on the kinetics data in which the statistical weight was set to be $1/\sigma^2$, where σ was the standard deviation of variables.

To calculate the total concentration of CO_2 released from decarboxylation of the anions, the equilibrium reactions 2 and 3 of CO_2 in solution have to be taken into account.[13]

$$CO_2 + H_2O \overset{K_{a1}}{\rightleftharpoons} H_3O^+ + HCO_3^- \quad (2)$$

$$HCO_3^- + H_2O \overset{K_{a2}}{\rightleftharpoons} H_3O^+ + CO_3^{2-} \quad (3)$$

The mass balance for the total CO_2 concentration is given by eq 4, where $[CO_2]_{free}$ is the CO_2 concentration based on the symmetrical absorption band due to asymmetric stretching at 2343 cm^{-1}.

$$[CO_2]_t = [CO_2]_{free} + [HCO_3^-] + [CO_3^{2-}] \quad (4)$$

$$= [CO_2]_{free}\left(1 + \frac{K_{a1}}{[H^+]} + \frac{K_{a1}K_{a2}}{[H^+]^2}\right)$$

Although Henry's law guaranteed that all of the released CO_2 was dissolved in the aqueous solution in hydrothermal solutions at high temperature and pressure, this was further indicated by the fact that we did not observe any gaseous CO_2, which has distinctive P and R rotational branches. The observed band intensity (or concentration) of CO_2 depends on the pH of the solution. The equilibrium constants K_{a1} and K_{a2} were calculated at high temperatures using the iso-Coulombic extrapolation method.[14] The ionization constant and specific volume of water at high temperatures needed in the iso-Coulombic extrapolation were calculated using the data of Marshall and Franck[15] and Uematsu and Franck.[16]

In addition to the real-time flow-reactor kinetics experiments, batch mode experiments of hydrothermolysis were conducted in order to characterize the reactions. A Ti tube with an internal volume of 12 cm^3 was sealed with the same aqueous solutions prepared for the flow reactor and then heated in a fluidized sand bath for the desired length of time. The amount of solution used was based on the specific volume of water, in order that the solution completely fill the tube at the reaction temperature. The tube was then cooled in a water bath to quench the reaction, and opened. In the case of $CF_3CO_2^-$, ^{19}F and ^1H NMR spectroscopy and F^- electrochemistry of the cooled solution were also conducted. Because of the basicity of solutions of lithium propiolate and cyanoacetate, a white precipitate (Li_2CO_3) was found to form, which would plug the flow reactor. A similar problem arose with lithium trifluoroacetate, but in this case the precipitate was LiF. For this reason, lower temperatures and shorter residence times were selected for kinetics experiments involving these compounds in order to reduce the potential for plugging of the reactor.

The concentration of F^- was measured in quenched solutions of 0.25 *m* CF_3CO_2M (M = Li, Na) that had been heated to 200−260 °C for 5 to 30 min by means of a ThermoOrion model 94−09 fluoride electrode and an Accumet model 25 pH/ion meter. NaF was used to prepare standards to create a ln $[F^-]$ vs mV calibration plot. Total Ion Strength Adjuster Buffer (ThermoOrion) was added to both the sample and standard and an adjustment was made to account for the dilution of F^-. All measurements were made using polyethylene beakers, and the solutions were stirred at the same rate using a Teflon coated magnetic stirring bar.

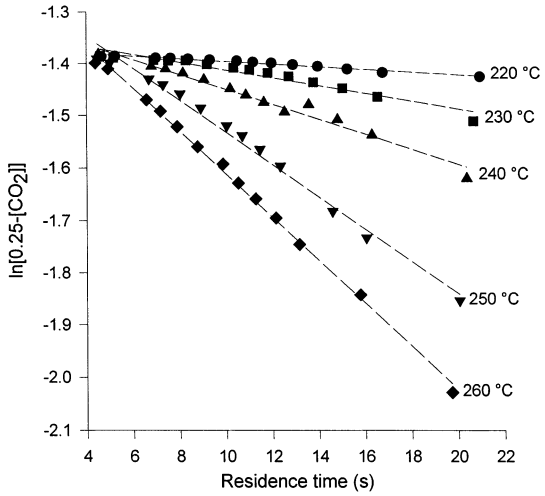

Figure 1. Rate plot for the decarboxylation of 0.25 M $K[CF_3CO_2]$ at the temperatures shown and 275 bar pressure (reaction 5). The basis is CO_2 production.

Results

Hydrothermolysis of $M[CF_3CO_2]$ Salts. The presence of halocarbons in water is of concern because of their deleterious effect on the environment. Removal of halocarbons from waste streams by the use of hydrothermal methods has motivated several studies.[17−19] We chose to study $CF_3CO_2^-$ because of its high solubility in water and the fact that few compounds containing C−F bonds have been studied at hydrothermal conditions. CF_3CO_2H is the strongest carboxylic acid and, therefore, it exists mostly as $CF_3CO_2^-$ with counterions in water. The effect of metal counterions on the decarboxylation rate of $CF_3CO_2^-$ might therefore be an important phenomenon.

The hydrothermal behavior of $CF_3CO_2^-$ proved to be a two-pronged problem. The decarboxylation reaction 5 occurred but was followed by the decomposition of CF_3H according to reactions 6 and 7.

$$M[CF_3CO_2] + H_2O \rightarrow CF_3H + CO_2 + M^+ + OH^- \quad (5)$$

$$CF_3H + 3OH^- \rightarrow HCO_2^- + 3F^- + H^+ + H_2O \quad (6)$$

$$HCO_2^- + H_2O \rightarrow CO_2 + H_2 + OH^- \quad (7)$$

To address the relative roles of reactions 5−7 in the overall behavior of $CF_3CO_2^-$, we measured the rate of CO_2 formation in real time using a flow-reactor with IR spectroscopy and designed a series of supporting ^1H and ^{19}F NMR spectral, F^- electrochemical, and pH measurements on the products from postreaction solutions from the tube reactor.

In situ measurements with IR spectroscopy using the Ti flow reactor were used to determine the initial decarboxylation rates (reaction 5) of $M[CF_3CO_2]$, where M = Group 1 cations. Conversion up to 40% based on the rate of formation of CO_2 was used and was found to follow a first-order (or pseudo first-order) rate law as the data in Figure 1 show. The rate of CO_2

TABLE 1: Rate Constants and Arrhenius Parameters for Decarboxylation of M[CF_3CO_2] (M = Li, Na, K, Rb, Cs)

temp °C	k s^{-1} ($\times 10^4$)	E_a kJ·mol^{-1}	ln(A) s^{-1}	$\Delta S^{\ddagger}$ J·K^{-1}·mol^{-1}
Li trifluoroacetate (0.25 *m*)		179.7 ± 16.8 (210−250 °C)[a]	37.4 ± 4.1	53
200	5.1 ± 1.2			
210	7.2 ± 0.6			
220	15.2 ± 0.4			
230	38.2 ± 0.3			
240	85.5 ± 0.3			
250	170.1 ± 0.6			
Na trifluoroacetate (0.25 *m*)		159.7 ± 6.0 (200−260 °C)[a]	32.43 ± 1.4	12
200	3.6 ± 0.4			
210	5.7 ± 0.3			
220	15.6 ± 0.3			
230	34.0 ± 0.2			
240	74.6 ± 0.2			
250	156.8 ± 0.4			
260	253.9 ± 0.4			
K trifluoroacetate (0.25 *m*)		157.9 ± 15.7 (220−240 °C)[a]	32.5 ± 3.8	13
210	10.4 ± 0.2			
220	27.1 ± 0.3			
230	60.7 ± 0.4			
240	113.1 ± 0.3			
250	216.2 ± 0.2			
260	274.3 ± 0.3			
270	404.0 ± 0.2			
280	488.5 ± 0.3			
Rb trifluoroacetate (0.25 *m*)		215.6 ± 33.5 (220−240 °C)[a]	45.8 ± 8.0	122
220	12.7 ± 0.6			
230	39.4 ± 0.6			
240	90.8 ± 0.5			
250	157.6 ± 0.4			
260	248.1 ± 0.4			
Cs trifluoroacetate (0.25 *m*)		190.0 ± 31.3 (220−240 °C)[a]	39.7 ± 7.5	72
220	13.4 ± 0.4			
230	39.1 ± 0.4			
240	84.8 ± 0.3			
250	152.9 ± 0.3			
260	247.8 ± 0.3			
270	295.4 ± 0.2			

[a] Temperature range considered for calculation of Arrhenius parameters.

formation was converted into the rate of decomposition of $CF_3CO_2^-$ by subtraction of the CO_2 concentration at each time from the initial $CF_3CO_2^-$ concentration. Table 1 gives the resulting rate constants. Discussed below is the fact that CO_2 formed in reaction 7 appears much more slowly and can be ignored at this stage of the reaction.

The CF_3H product of reaction 5 slowly reacts at 200−260 °C and 275 bar according to reaction 6. The presence of CF_3H was clearly confirmed by ^{19}F NMR spectroscopy, but quantitation of CF_3H is not reliable because of loss due to its high vapor pressure and poor solubility in water. The presence of HCO_2^- was confirmed by the use of ^1H NMR spectroscopy of the aqueous solution of $CF_3CO_2^-$ that had been heated in a tube reactor at 260 °C for 15 min. F^- was also clearly detected by ^{19}F NMR spectroscopy. There were no ^{19}F signals for other species such as CH_2F_2 or CH_3F. The rate of reaction 6 could not be determined in the flow reactor because none of the species absorb in the IR band-pass of the sapphire windows. Therefore, the rate of reaction 6 was obtained by measuring the concentration of F^- by the use of electrochemistry on solutions of $CF_3CO_2^-$ heated at 200−260 °C in the tube reactor for the times shown in Table 2. The F^- concentrations can be converted to the corresponding amount of $CF_3CO_2^-$ that had to have decomposed, and these values are shown in Table 2. Table 2 also shows the resulting rate constants for removal of $CF_3CO_2^-$ based on F^- production. By comparing the 260 °C data in Tables 1 and 2, it can be determined that only about 4% of the $CF_3CO_2^-$ has produced F^- (through reaction 6 in the Ti tube) after 5 min, whereas 40% of the $CF_3CO_2^-$ has converted to CO_2 in 40 s. Thus reaction 5 is much faster than reaction 6. For a more general view, the rates of disappearance of $CF_3CO_2^-$ based on CO_2 and F^- production from Na[CF_3CO_2] are compared in the Arrhenius plot shown in Figure 2. Since F^- production requires both reactions 5 and 6, and reaction 6 occurs more slowly, the overall rate of F^- formation is slower than CO_2 production, which requires only reaction 5.

The pH of the solutions from the tube reactions gave additional support for reactions 5−7. Figure 3 shows that the solution is more basic at shorter reaction times, as might be expected from the OH^- production by reaction 5, but became less basic as the reaction progressed because of the gradual consumption of OH^- by reaction 6. When the F^- concentration in the Na[CF_3CO_2] solution was followed, reaction 6 slowed at longer times in part because the H^+ formed decreased the pH. Higher [OH^-] may facilitate the decomposition reaction of CF_3H according to reactions 8 and 9. Nucleophilic attack by OH^- at the carbon atom of CF_3^- is plausible based on the fact that a Hartree−Fock SCF level calculation of the CF_3^- ion indicated that the charge on the carbon atom is +0.5e.

$$CF_3H + OH^- \rightarrow CF_3^- + H_2O \quad (8)$$

$$CF_3^- + 2OH^- \rightarrow HCO_2^- + H^+ + 3F^- \quad (9)$$

The rate of reaction 7 is known from previous measurements in a Ti flow cell.[20] The rate of reaction 7 was extrapolated from the higher temperature regime of measurement into that determined here for reactions 5 and 6. Considered together, the rates of reactions 5−7 follow the order 5>6>7, as is shown in Figure 2. At longer reaction times the solution becomes slightly more basic (Figure 3), perhaps because of reaction 7.

Whether the F^- might result from direct defluorination of $CF_3CO_2^-$ rather than CF_3H is partially answered by the faster rate of formation of CO_2 compared to F^-. Additional evidence that CF_3H is the source of F^- was obtained by comparing the integrated intensities of F^- and $CF_3CO_2^-$ in the ^{19}F NMR spectrum, which are shown in Figure 4. Notice that most of the $CF_3CO_2^-$ has disappeared before the F^- ion is observed.

Conversion of the rates for reaction 5 into an Arrhenius plot for the salts of $CF_3CO_2^-$ yielded Figure 5. Within the 95% confidence interval shown, all of the salts behave in the same manner. However, the individual Arrhenius plots shown in Figure 5 reveal that the Li^+ and Na^+ salts are linear in the temperature range studied, whereas those of K^+, Rb^+, and Cs^+ are curved and become less dependent on the temperature at higher temperatures. The hypothesized explanation for the curvature in the Na^+, K^+, and Rb^+ salt data is as follows: The production of F^- by reaction 6 presents the opportunity to form insoluble MF salts because the bulk dielectric constant of H_2O is lower at higher temperature. Both ion pair formation and precipitation of MF are expected in the order $Li^+ > Na^+ > ... > Cs^+$, that is, in the order of increasing ionic potential of the cation. However, only LiF was observed to precipitate in the batch reaction work. LiF also precipitated in the flow reactor resulting in plugging at higher temperatures. While NaF precipitate was not observed, considerable ion pairing is

TABLE 2: Calculated Values for $[CF_3CO_2Na]_t$ and Rate Constants Based on Electrode Measurements of $[F^-]_t$

reaction time (min)	$[CF_3CO_2Na]_t$[a]						
	200 °C	210 °C	220 °C	230 °C	240 °C	250 °C	260 °C
5	0.25	0.2499	0.2501	0.2489	0.248	0.2449	0.2398
10	0.25	0.2497	0.2496	0.2469	0.2444	0.2388	0.2322
15	0.2499	0.2496	0.2489	0.2448	0.2396	0.2357	0.2295
20	0.2499	0.2493	0.2479	0.2431	0.2378	0.2335	0.2276
25	0.2498	0.2491	0.2478	0.2418	0.2363	0.2323	0.2248
30	0.2497	0.2487	0.2465	0.24	0.2358	0.2305	0.2251
k, s^{-1} ($\times 10^4$)	0.20 ± 0.49	1.31 ± 0.72	3.66 ± 0.65	11.97 ± 0.83	12.44 ± 0.60	15.84 ± 0.64	21.33 ± 0.70

[a] $[CF_3CO_2Na]_t = \{[CF_3CO_2Na]_0 - ([F^-]_t/3)\}$.

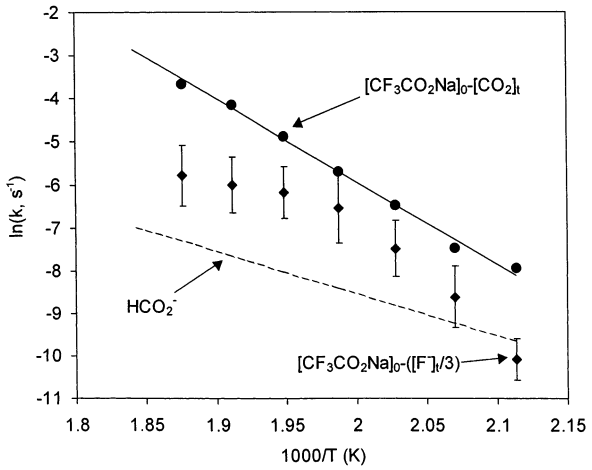

Figure 2. Arrhenius plots comparing the rate constants of decomposition of $Na[CF_3CO_2]$ based on F^- (electrochemistry), which is indicative of reaction 6, and CO_2 (flow reactor) production, which is related to reaction 5. Also shown are extrapolated rate constants for reaction 7 (HCO_2^-).

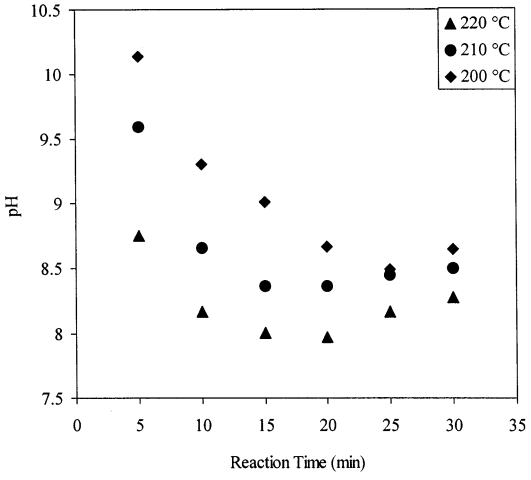

Figure 3. The change in pH (measured at 25 °C) of the quenched solution from the Ti tube reaction of aqueous $Na[CF_3CO_2]$ undergoing reactions 5−7. The trend observed is consistent with the progress of the reaction.

expected at the hydrothermal conditions used. Thus, kinetic data for the Li^+ and Na^+ salts could not be obtained in the highest temperature range. The rates in Figure 5 are seen to have decreasing temperature dependence at higher temperature for the K^+, Rb^+, and Cs^+ salts, perhaps because less ion pairing with F^- enables the effective ionic strength to increase faster during the reaction. This hypothesis was supported by separate experiments that showed that higher ionic strengths obtained by the addition of excess KF to the reaction mixture reduced the decarboxylation rate of aqueous $K[CF_3CO_2]$ (Figure 6). Even clearer evidence that removal of F^- ions from the solution occurs

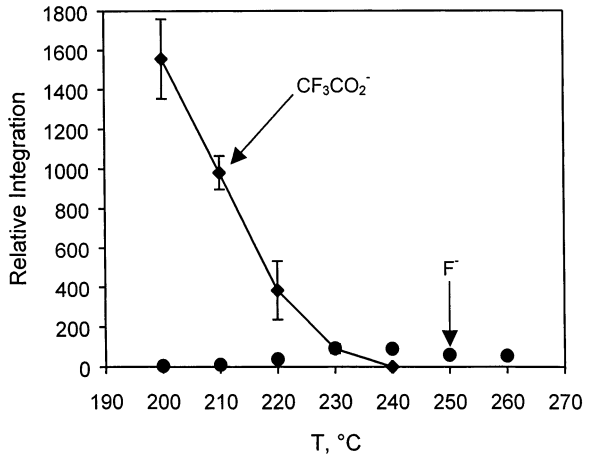

Figure 4. The integrated ^{19}F NMR signal intensity for aqueous $Li[CF_3CO_2]$ showing that most of the $CF_3CO_2^-$ has disappeared before the F^- appears. This is evidence that F^- does not come directly from $CF_3CO_2^-$. The error bars and F^- are within the size of the data points.

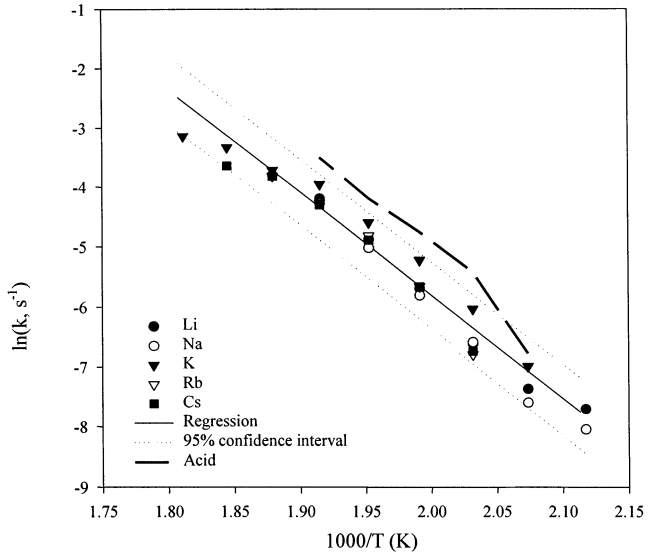

Figure 5. Arrhenius plots for the decarboxylation of the Group 1 cation salts of $CF_3CO_2^-$ based on CO_2 production showing the 95% confidence interval.

in the order $Li^+ > Na^+$ was obtained by comparing the F^- concentration from electrochemical analysis of the $CF_3CO_2^-$ salts of Li^+ and Na^+ obtained from the batch mode decomposition. These results are shown in Figure 7. At higher temperatures the LiF begins to precipitate, thus lowering the free F^- concentration, whereas the concentration of F^- from the Na^+ salt increases with temperature but at a decreasing rate. The reduction of the decarboxylation rate as the ionic strength of the solution is increased has also been observed with other acids, such as the amino acid alanine.[21]

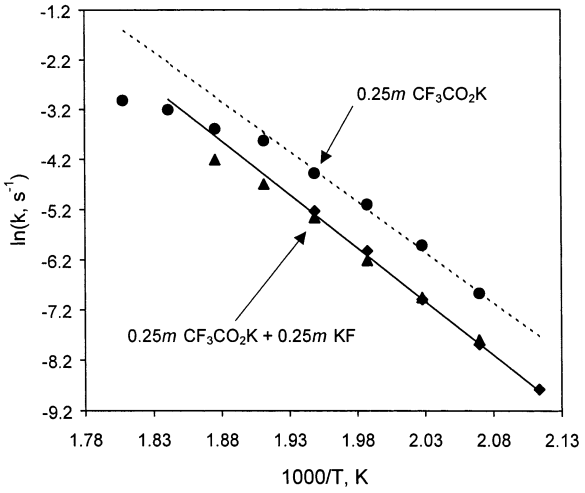

Figure 6. Arrhenius plot showing that the addition of 0.25 *m* KF to 0.25 *m* K[CF_3CO_2] slows down the decarboxylation rate. The dashed line fits the four lowest temperature data points to emphasize the curvature at the higher temperatures.

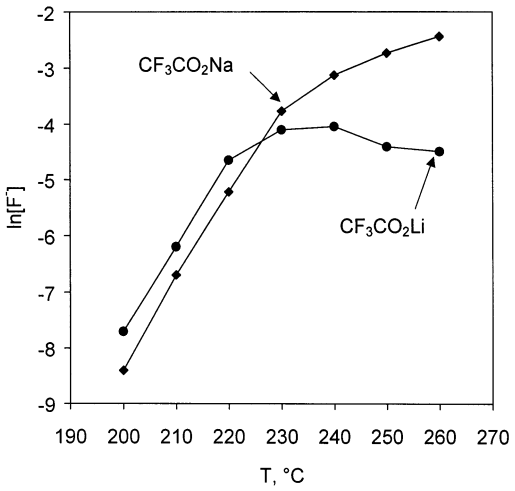

Figure 7. The F^- concentration from the electrochemical measurements of aqueous solutions of the Li^+ and Na^+ salts of $CF_3CO_2^-$ showing that F^- is removed at higher temperatures in the order $Li^+ > Na^+$ due to MF association.

Based on the observations above, the transition state for decarboxylation would appear to be less polar than the reactant. A more theory-based assessment on the polarity of the transition state can be made based on the Kirkwood analysis (eq 10), which takes into account Coulombic interactions, dipole moments, radii, and the dielectric constant of the medium as they apply to kinetics.[22]

$$\ln k_H = \ln k_0 + \frac{N}{RT}\left(\frac{\epsilon - 1}{2\epsilon + 1}\right)\left(\frac{\mu_{TS}^2}{r_{TS}^3} - \frac{\mu_A^2}{r_A^3} - \frac{\mu_B^2}{r_B^3}\right) \quad (10)$$

where k_H is the hydrolysis constant at temperature T, k_0 is the rate constant in a hypothetical medium having $\epsilon = 1$, and μ and r are the dipole moment and radii of reactants A, B, and the transition state (TS). Equation 10 has been treated in a way that does not require knowledge of the dipole moments and radii of the reactants and the transition state.[23] Equation 10 has the form of the equation of a straight line. Therefore, if ln k_0 is taken to be the y intercept and N/RT is constant, then a plot of ln k_H vs $(\epsilon - 1/2\epsilon + 1)$ will result in a line with slope $(\mu_{TS}^2/r_{TS}^3 - \mu_A^2/r_A^3 - \mu_B^2/r_B^3)$. For reactions with transition states that are less polar than the reactants, the slopes should be negative. If the slope is negative, the $(\mu_{TS}^2/r_{TS}^3 - \mu_A^2/r_A^3 - \mu_B^2/r_B^3)$ portion of eq 10 must also be negative. This can be possible only if the dipole moments of reactants A and B are larger than that of the transition state. Figure 8 is a plot of ln k_H vs $(\epsilon - 1/2\epsilon + 1)$ for the five alkali metal salts of $CF_3CO_2^-$. In all five cases the slopes are negative, confirming that the transition state formed during the heterolytic cleavage of the C−C bond is less polar than the reactants.

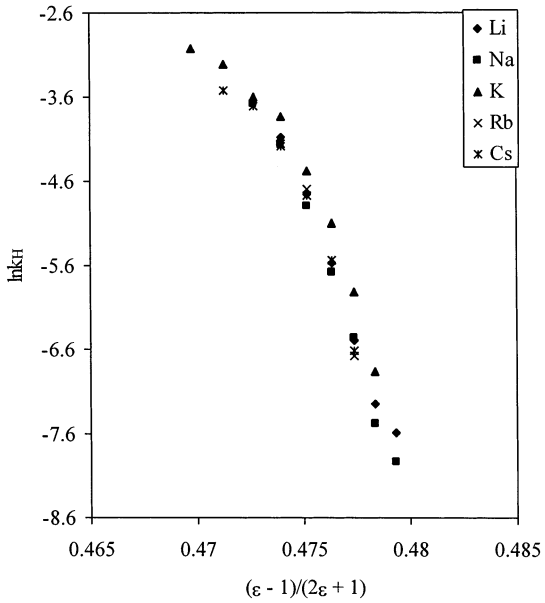

Figure 8. Plot based on the Kirkwood eq 9. All five alkali metal salts of $CF_3CO_2^-$ exhibit a negative slope which is indicative of a transition state that is less polar than the reactants.

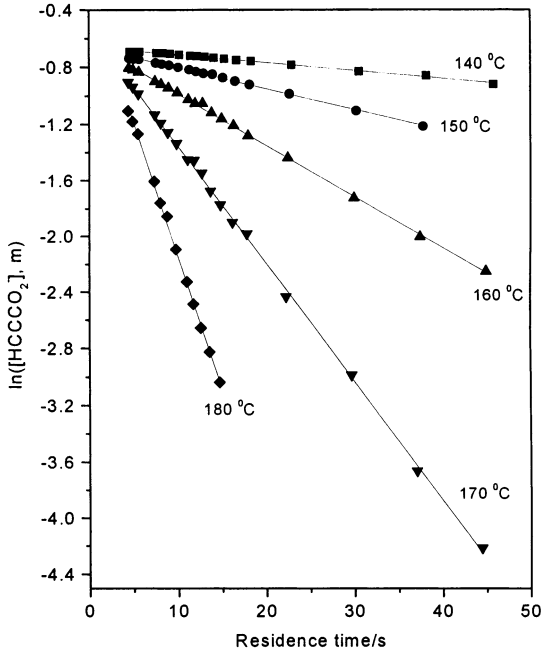

Figure 9. First-order rate plot for decarboxylation of 0.5 *m* K[$HCCCO_2$] at 275 bar.

Hydrothermolysis of M[$HCCCO_2$] Salts. The hydrothermolysis of propiolic acid has been investigated recently.[24] Propiolic acid is a weaker acid than trifluoroacetic acid. However, by using the iso-Coulombic extrapolation method, only 0.02% of the 0.5 *m* propiolate ion is converted to the

TABLE 3: Rate Constants and Arrhenius Parameters for Decarboxylation of Propiolate Salts

temp °C	k s^{-1} ($\times 10^3$)	E_a kJ·mol^{-1}	ln(A) s^{-1}	$\Delta S^{\ddagger}$ J·K^{-1}·mol^{-1} [a]
Li propiolate (0.5 *m*)		146.8 ± 2.9	37.1 ± 0.8	52
140	3.6 ± 0.3			
150	9.6 ± 0.3			
160	26.7 ± 0.7			
170	64.1 ± 1.5			
Na propiolate (0.5 *m*)		133.9 ± 2.8	33.7 ± 0.8	23
140	5.0 ± 0.1			
150	13.4 ± 0.3			
160	31.7 ± 0.7			
170	68.7 ± 1.1			
180	169.8 ± 4.8			
K propiolate (0.5 *m*)		136.6 ± 1.5	34.6 ± 0.5	31
140	5.5 ± 0.1			
150	14.8 ± 0.2			
160	36.5 ± 0.3			
170	83.9 ± 0.6			
180	183.6 ± 4.8			
Rb propiolate (0.5 *m*)		133.8 ± 2.3	33.9 ± 0.6	25
140	5.5 ± 0.1			
150	15.7 ± 0.2			
160	38.4 ± 0.4			
170	84.3 ± 1.2			
180	191.1 ± 1.9			
Cs propiolate (0.5 *m*)		134.5 ± 1.6	34.1 ± 0.5	26
140	5.8 ± 0.1			
150	15.8 ± 0.2			
160	37.1 ± 0.5			
170	85.8 ± 1.0			
180	192.1 ± 2.9			
propiolate anion [b]		134.70 ± 1.1	34.1 ± 0.3	

[a] Calculated at average temperature. [b] Excludes Li^+ data.

neutral propiolic acid at temperature 200 °C, and therefore propiolic acid need not be considered further in the calculation.

The IR spectra for the decarboxylation of propiolate anion at 275 bar and temperature range from 140 to 190 °C were based on the disappearance of the 2090 cm^{-1} band due to the C≡C of propiolate. The C≡C stretching mode of the C_2H_2 product of decarboxylaton is of course IR inactive. Figure 9 shows the rate plot for the decarboxylation of 0.5 *m* potassium propiolate solution at 275 bar, which indicates that the decarboxylation process is pseudo-first-order. The rate constants with different counterions and Arrhenius parameters are given in Table 3. The effect of the counterions on the decarboxylation rate is displayed in Figure 10, where a plot of the rate constants versus the ion radii[25] in aqueous solution is shown. It can be seen that the rate constant of decarboxylation increases with the enlargement of ion radius of counterion, but Table 3 reveals that the mean value activation energy and frequency factor for the Na^+, K^+, Rb^+, and Cs^+ salts are not significantly different. The Li^+ salt is, however, significantly different and produces a lower rate of decomposition.

M[NCCH$_2$CO$_2$]. The decarboxylation kinetics of cyanoacetic acid and its anion have been studied in our previous work,[9] where the decarboxylation reaction 11 was clearly seen from the spectra at different temperatures (Figure 11). Less than 1% of the cyanoacetate ion hydrolyzes to the acid at 200 °C so that the acid contribution can be ignored.

$$N{\equiv}CCH_2CO_2^- + H_2O \rightarrow CH_3C{\equiv}N + CO_2 + OH^- \quad (11)$$

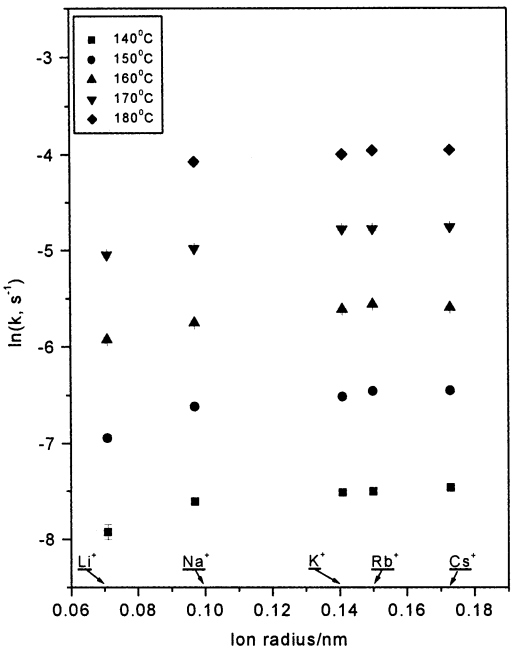

Figure 10. Effect of the Group 1 cations on the decarboxylation rate of $HCCCO_2^-$ at various temperatures.

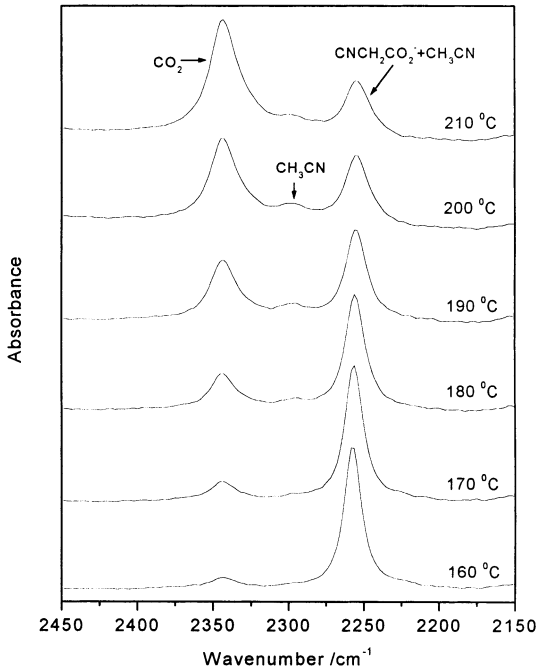

Figure 11. IR spectra for Na[$NCCH_2CO_2$] from the flow reactor at 275 bar showing the nitrile overlap region and CO_2 formation.

The kinetics of reaction 11 were calculated from the observed C≡N band of $NCCH_2CO_2^-$. However, the product CH_3CN has two bands located at 2297 and 2257 cm^{-1}. The band at 2257 cm^{-1} overlapped the 2254 cm^{-1} band of the reactant nitrile. Therefore, the CH_3CN contribution to the band area of 2254 cm^{-1} must be removed to obtain the concentration of $NCCH_2CO_2^-$. The hydrolysis of CH_3CN to acetamide and then to acetic acid is slow in neutral hydrothermal solution even at 300 °C and can be assumed to be negligible[26] within the error limits of the kinetic experiments. Nevertheless, the absorptivity of CH_3CN decreased with increasing temperature in the 100−330 °C range at 275 bar according to flow reactor IR spectroscopy. This changing absorptivity, which is not due to reaction of CH_3CN, was taken into account to reduce the uncertainty in

TABLE 4: Rate Constants and Arrhenius Parameters for Decarboxylation of Cyanoacetate Salts

temp °C	k s^{-1} ($\times 10^3$)	E_a kJ·mol^{-1}	ln(A) s^{-1}	$\Delta S^{\ddagger}$ J·K^{-1}·mol^{-1}
Li cyanoacetate (0.25 *m*)		143.5 ± 8.5	32.5 ± 2.2	13[a]
160	0.6 ± 0.1			
170	1.3 ± 0.1			
180	3.7 ± 0.1			
190	9.2 ± 0.2			
200	19.3 ± 0.5			
210	32.8 ± 1.0			
Na cyanoacetate (0.25 *m*)		145.8 ± 4.1	33.1 ± 1.1	17
160	0.5 ± 0.1			
170	1.4 ± 0.04			
180	3.8 ± 0.1			
190	8.9 ± 0.2			
200	18.3 ± 0.5			
210	36.6 ± 1.3			
K cyanoacetate (0.25 *m*)		141.9 ± 4.5	32.1 ± 1.2	10
160	0.51 ± 0.03			
170	1.7 ± 0.1			
180	3.8 ± 0.1			
190	9.1 ± 0.1			
200	18.4 ± 0.4			
210	37.4 ± 0.8			
Rb cyanoacetate (0.25 *m*)		141.3 ± 6.3	31.9 ± 1.6	8
160	0.56 ± 0.03			
170	1.39 ± 0.05			
180	4.0 ± 0.1			
190	9.7 ± 0.2			
200	18.4 ± 0.3			
210	35.6 ± 0.8			
Cs cyanoacetate (0.25 *m*)		143.5 ± 4.4	32.5± 1.2	13
160	0.53 ± 0.04			
170	1.50 ± 0.04			
180	3.8 ± 0.1			
190	9.0 ± 0.1			
200	18.4 ± 0.4			
210	36.1 ± 1.1			
cyanoacetate anion[c]		143.2 ± 2.6	32.2 ± 0.7	

[a] Calculated at average value of temperature range.

the concentration calculation. The process was divided into three steps. First, the total CO_2 concentration was calculated from the observed CO_2 concentration using the $[H^+]$ of initial solutions at each temperature and residence time. Second, according to eq 11, the concentration of CH_3CN is equal to that of the total CO_2 concentration, which enabled the band areas of CH_3CN to be converted to concentrations at each temperature and residence time. Finally, the band areas of reactant $NCCH_2CO_2^-$ were obtained by subtracting the CH_3CN band area from the total band area centered at 2254 cm^{-1}. After this correction, the calculated rate constants were found to be the same within the uncertainty of the measurement. The obtained rate constants are given in Table 4 for the decarboxylation of the cyanoacetate ion with different counterions. The effect of the ion radius on the decarboxylation rate is shown in Figure 12. No significant effect was observed.

Hydrothermolysis of M[$O_2CCH_2CO_2H$] Salts. A previous kinetic study of the rate of decarboxylation of M[$O_2CCH_2CO_2H$] salts M = Li, Na, K, Rb, Cs also revealed some curvature in the Arrhenius plots at higher temperatures.[6] The data show that the rate increases with increasing cation size, with the possible exception of Rb^+.[6,27] The sensitivity of the rate of the malonate salts to the cation contrasts with the $CF_3CO_2^-$ salts, which were

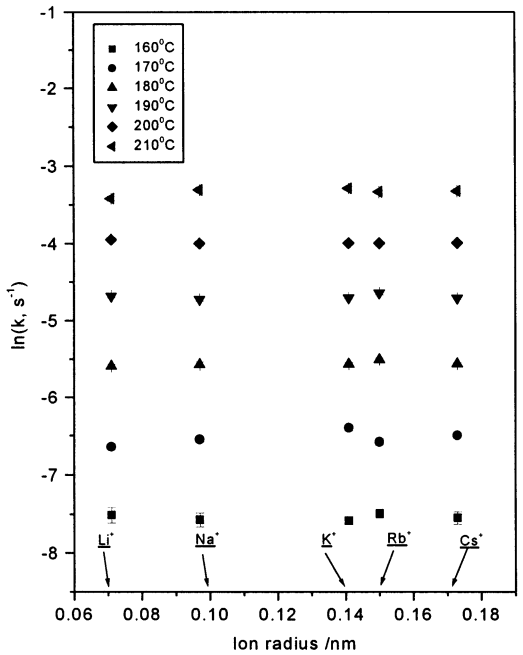

Figure 12. Effect of the Group 1 cations on the decarboxylation rate of $NCCH_2CO_2^-$ at various temperatures.

shown in Figure 5 to have the same rate within the 95% confidence interval at the conditions used.

Discussion of Counterion Effects. Careful studies of the rates of decarboxylation of carboxylate ions uncover the fact that the Group 1 cations can influence the rate of decomposition in a variety of ways. Although the differences are not large, each of the four anions studied behaves slightly differently. Therefore, the counterion effects would appear to have many origins and therefore be difficult to predict without guidance from experimental data.

The mechanism of decarboxylation of carboxylic acids and carboxylates in aqueous solution is often accepted[28] to be similar to that of S_N2 nucleophilic bimolecular substitution. In aqueous solution, water molecules act as the nucleophile, making the observed rate constant pseudo-first-order. First, the nucleophile attacks the carbonyl carbon atom, followed by the loss of carbon dioxide and the formation of the carbanion by heterolytic cleavage. The activated complex is formed by initial nucleophilic attack on the carbonyl carbon atom. The carbanion picks up H^+ to form the neutral species, in this case CF_3H. An analogous mechanism involving ion pairing[29] that may be more relevant to the carboxylate salts involves two transition states. The first is the formation of contact ion pairs and the second is the formation of an activated complex by nucleophilic attack of water molecules on the ion pair. If formation of the first transition state is rate-determining, then the global decarboxylation process is a unimolecular reaction. In accordance, the entropies of activation in Tables 1, 3, and 4 tend to be positive. If formation of the second transition state is rate-determining, then the reaction should be bimolecular. Countercations having the highest ionic potential might stabilize the carbanions formed by heterolytic cleavage in the decarboxylation process involving the ion pair mechanism because they form contact ion pairs or solvent separated ion pairs more efficiently at hydrothermal conditions. As a result, smaller counterions might be expected to increase the rate constant.

There are several problems with the present data in the scenerio given above. For example, the rate of decarboxylation of the cyanoacetate anion with different counterions revealed

only small variation with the choice of the counterion. Thus, in the trifluoroacetate anion, where the ion pairing between CF_3^- and M^+ should be greatest, Li^+ instead retards the rate of decarboxylation. The decarboxylation rate of the trifluoroacetate anion is mostly affected by the secondary ionic strength effect in which F^- is complexed by the cation. The addition of KF to the trifluoroacetate retarded the reaction rate (Figure 6). In the propiolate anion, only the Li^+ ion affects the rate differently from the other ions and retards the decarboxylation reaction. In the malonate anion, there is a more or less systematic trend of decreasing rate with increasing ionic potential of the cation.

These differences can be understood better by hypothesizing slightly different reasons for the counterion effect in accordance with the experimental findings. Indeed, the ion association concept can be retained in all cases, but with detailed differences that depend on the carboxylate ions. The behavior of the $CF_3CO_2^-$ ion is a somewhat special case in that the cation effect appears to result primarily from the change of ionic strength of the solution during the reaction. As the F^- ions form as a result of secondary decomposition of the CF_3H product, they remove the Li^+ ions by precipitation and the Na^+ ions by ion pairing. This leads to less influence by the salt effect for the Li^+ and Na^+ salts compared to the K^+, Rb^+, and Cs^+ salts. The decarboxylation rate of trifluoroacetate salts of the latter three ions therefore increases less rapidly at high temperature. In the case of propiolate, only the Li^+ ion affects the rate compared to the other Group 1 cations. Since Li^+ has the highest ionic potential, it can associate most strongly with the $HCCCO_2^-$ ion as in structure I. Stabilization of this ion pair may involve the resonance form II, which strengthens the $C-CO_2$ bond and slightly reduces the decarboxylation rate.

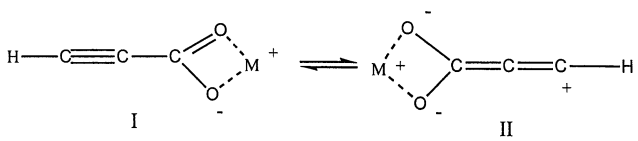

I II

In the case of the $NCCH_2CO_2^-$ ion the resonance form II does not exist and hence the cation has little effect on the decarboxylation rate. In the case of malonate, where there exists a systematic difference in the decarboxylation rate depending on the cation, the probable reason is that the transition state may be different from the other anions studied. For the malonate ion the transition state is likely to be a six-member ring structure which facilitates the proton-transfer step essential to decarboxylation. Thus, when $M = H^+$, the rate of decarboxylation is the fastest and any species that competes with H^+ for the position in the ring will reduce the decarboxylation rate.[6] When M is a Group 1 cation, M^+ competes with H^+ for the position in the ring in the order $Li^+ > Na^+ > K^+$. Hence, the rate of decarboxylation of the Li^+ salt is the lowest.

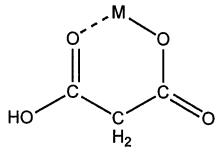

III

Acknowledgment. We are grateful for support of this work by the National Science Foundation on CHE-9807370 and the Army Research Office on DAAG55-98-1-0253.

References and Notes

(1) Shock, E. L.; Korestky, C. M. *Geochim. Cosmochim. Acta* **1993**, *57*, 4899.
(2) Shock, E. L.; Korestky, C. M. *Geochim. Cosmochim. Acta* **1995**, *59*, 1497.
(3) Sverjensky, D. A.; Shodi, E. L.; Helgeson, H. C. *Geochim. Cosmochim. Acta* **1997**, *61*, 1359.
(4) Bell, J. L. S.; Palmer, D. A.; Barnes, H. L.; Drummond, S. E. *Geochim. Cosmochim. Acta* **1994**, *58*, 4155.
(5) Belsky, A. J.; Maiella, P. J.; Brill, T. B. *J. Phys. Chem. A* **1999**, *103*, 4253.
(6) Gunawardena, N. R.; Brill, T. B. *J. Phys. Chem. A* **2001**, *105*, 1876.
(7) Kieke, M. L.; Schoppelrei, J. W.; Brill, T. B. *J. Phys. Chem*. **1996**, *100*, 7455.
(8) Schoppelrei, J. W.; Kieke, M. L.; Wang, X.; Klein, M. T.; Brill, T. B. *J. Phys. Chem.* **1996**, *100*, 14343.
(9) Belsky, A. J.; Maiella, P. G.; Brill, T. B. J. *Phys. Chem*. A **1999** *103*, 4253.
(10) Brill, T. B. J. *Phys. Chem.* A **2000**, *104*, 4343.
(11) Maiella, P. G.; Schoppelrei, J. W.; Brill, T. B. *Appl. Spectrosc.* **1999**, *53*, 351.
(12) Cvetanovic, R. J.; Singleton, D. L. *Int. J. Chem. Kinet*. **1977**, *9*, 481.
(13) Butler, J. N. *Ion Equilibrium, Solubility and pH Calculation*; John Wiley & Sons: New York, 1998; p 368.
(14) Lindsay, W. T. *Proc. Int. Water Conf. Eng. Soc. W. Pa*. **1980**, *41*, 284.
(15) Marshall, W. L.; Franck, E. U. *J. Phys. Chem. Ref. Data* **1981**, *10*, 295.
(16) Uematsu, M.; Franck, E. U. *J. Phys. Chem. Ref. Data* **1980**, *9*, 1291.
(17) Houser, T. J.; Liu, X. *J. Supercrit. Fluids* **1996**, *9*, 167.
(18) Park, S. W.; Yoon, J. H.; Lee, H. *Korean J. Chem. Eng.* **1996**, *13*, 640.
(19) Marrone, P. A.; Arias, T. A.; Peters, W. A.; Testor, J. W. *J. Phys. Chem. A* **1998**, *102*, 7013.
(20) Maiella, P. G.; Brill, T. B. *J. Phys. Chem. A* **1998**, *102*, 5886.
(21) Li, J.; Wang, X. G.; Klein, M. T.; Brill, T. B. *Int. J. Chem. Kinet*. **2002**, *34*, 271.
(22) Newman, K. E. *Chem. Soc. Rev.* **1994**, *23*, 31.
(23) Klein, M. T.; Torry, L. A.; Wu, B. C.; Townsend, S. H. *J. Supercrit. Fluids* **1990**, *3*, 222.
(24) Li, J.; Brill, T. B. *J. Phys. Chem. A* **2001**, *105*, 6171.
(25) Marcus, Y. *Chem. Rev.* **1988**, *88*, 1475.
(26) Izzo, B. H.; Klein M. T. *AIChE J.* **1997**, *43*, 2048.
(27) Brill, T. B.; Belsky, A. J.; Gunawardena, N.; Miksa, D. *High Press. Res.* **2001**, *20*, 429.
(28) Clark, L. W. In *The Chemistry of Carboxylic Acids and Esters. The Chemistry of Functional Groups Series*; Patai, S., Ed.; John Wiley: New York, 1969; p 589.
(29) Solomons, T. W. G. *Organic Chemistry*, 4th ed.; John Wiley & Sons: New York, 1988.